Effect of Stirring on Chemically Deposited ZnO Thin Films

M. Önal* and B. Altiokka
Bilecik Şeyh Edebali University, Bilecik 11210, Turkey

(Received January 29, 2020; in final form March 20, 2020)

In this study, the effects of stirring rate were investigated while ZnO thin films were produced by the chemical bath deposition method. Five different samples were produced by mixing the prepared solution at 0, 300, 600, 900, and 1200 rpm cycles. Scanning electron microscope showed that ZnO nanorods were formed very rarely when the solution was not stirred and that the nanorods became more frequent as the stirring rate increased. X-ray diffraction results showed that all films formed hexagonal wurtzite structure and peak intensities were compatible with the ASTM card. According to the absorbance measurements, the energy band gaps of the samples were between 3.02 eV and 3.97 eV. When the visualization of the obtained films was examined, it was observed that as the stirring rate increased, ZnO adhered well on the glass substrates. It was observed that the film adhering on the glass substrate at 0 rpm was very weak, whereas the film adhered very well on the glass surface as the solution stirring rate increased.

DOI: 10.12693/APhysPolA.137.1209
PACS/topics: ZnO, chemical bath deposition, stirring rate, thin film

1. Introduction

Nanocrystalline semiconductor materials are of great interest due to their size-dependent properties and wide application areas [1]. In particular, ZnO is a semiconductor material that attracts the attention of researchers with its n-type conductivity, 3.3 eV energy band gap, and potential applications. The potential uses of ZnO are piezoelectrical devices, chemical sensors, electroluminescent devices, solid-state emission, solar cells, transparent electrodes, photo-catalysts, and ultraviolet laser diodes [2–4]. The main reason for this interest is that zinc oxide (ZnO) is a versatile semiconductor with multifunctional properties that can be easily synthesized in various structural forms [5]. The development of high-quality ZnO thin films has been made possible by advances in deposition techniques. Some of these techniques are ultrasonic spray pyrolysis, chemical bath deposition, sol–gel, RF magnetron spray, precipitation in water solution, hydrothermal synthesis, pulse laser deposition [6–8]. Among all these methods, chemical bath deposition (CBD) is a highly preferred method because of its low cost, high efficiency, simplicity and compliance with large scale production [9].

In the literature, the effects of the stirring rate on the growth of CdS films produced by the chemical bath deposition method have already been investigated. In this mentioned experiment, CdS was obtained by mixing at 250, 350, 450 rpm, X-ray diffraction (XRD) peak densities increased and film thicknesses were 40, 80, and 120 nm, respectively [10]. In addition, Zhang et al. investigated various properties of ZnS films deposited at different stirring rates (150–525 rpm) by the CBD method. It was seen that when the stirring rates increased, the films' thickness also increased [11]. However, the effects of stirring on ZnO thin films have not been investigated in the literature.

In this study, the effects of stirring rate when producing ZnO thin films with chemical bath deposition were investigated for the first time. The stirring rate has significant effects on structural and surface morphology. These effects were investigated in detail.

The visual photos of the thin films reveal the effect of the stirring rate on the surface of samples. As can be seen from these photos, the film thickness increased with an increasing stirring rate. UV measurements showed that when the solution was not stirred, the absorbance values of the films were relatively low such as 0.45 and when stirred, absorbance value increased to 2.00 above the wavelength of 400 nm. It was observed that the energy bandgap of the films decreased from 3.97 eV to 3.02 eV.

2. Experimental details

In this study, the chemical bath deposition method was used to produce ZnO thin films. Before starting the deposition process, the bath container was washed with 10% HCl acid and the glass substrate was washed with acetone and rinsed with deionized water. After then, 100 ml deionized water was placed in the bath container and heating was started. In the bath container, when the deionized water temperature reached 30 °C, 65 mM $ZnCl_2$ and 6 mM EDTA were dissolved. The pH of the solution was adjusted to 10.25 using NaOH. While the first sample was being produced, the solution was heated to the 85 °C and the deposition was completed in 25 min. Besides, in this experiment, the solution was not stirred. This sample was named as rpm0.

*corresponding author; e-mail: metehan.onal@bilecik.edu.tr

TABLE I

The summarized details for ZnO experiment, where $Ph = 10.25$, temperature $T = 85 \pm 2\,^{\circ}\mathrm{C}$.

Exp.	$ZnCl_2$ [mM]	EDTA [mM]	Stirring rate [rev/min]
rpm0	65	6	0
rpm300	65	6	300
rpm600	65	6	600
rpm900	65	6	900
rpm1200	65	6	1200

Under the same conditions mentioned above, four other different samples were produced being stirred at 300, 600, 900, and 1200 rpm and the samples were named as rpm300, rpm600, rpm900, and rpm1200. Each sample was rinsed using pressurized water and allowed to dry at room temperature. All production conditions of the samples were given in Table I.

Optical properties of ZnO thin film samples were studied with JASCO V-530 with double beam UV-vis spectrometer. The morphological characteristic of the films was observed using a Zeiss SUPRA 40VP SEM. The crystal structure was examined using a PANalytical Empyrean XRD. For analysis of the Fourier transform infrared photometer (FTIR) a PERKIN Elmer device was used.

3. Results and discussion

3.1. Structural analysis of ZnO films

The thicknesses of the obtained samples were calculated by the gravimetric method. The thickness of the film obtained without stirring was calculated at an average of 175 nm and the other samples were calculated to be ≈ 650 nm. Since the metal ions in the solution are heavier than water molecules, when the solution was not mixed they precipitated to the bottom and did not participate in the chemical reaction. When the solution was stirred, since metal ions are heavier than water molecules, they were exposed to more centrifugal forces. Metal ions that were subjected to more centrifugal forces were directed to the glass surface, causing more reactions to occur on the glass substrate and increasing the film thicknesses.

The structural properties of ZnO thin films were investigated by using XRD. The XRD patterns are given in Fig. 1. As seen in Fig. 1, all films had a hexagonal structure. To calculate the preferred orientations of the films we used the following formula:

$$T.C. = \frac{I(hkl)}{I_0\,(hkl)} \Big/ \left[\frac{1}{N}\sum_N \frac{I\,(hkl)}{I_0\,(hkl)}\right], \tag{1}$$

where $I_0(hkl)$ is the standard density of the (hkl) plane given on the ASTM card, and $I(hkl)$ is the measured relative density of the (hkl) plane. Calculated texture coefficient values are given in Table II. There one can see that the preferred orientation has shifted from plane (010) to plane (002).

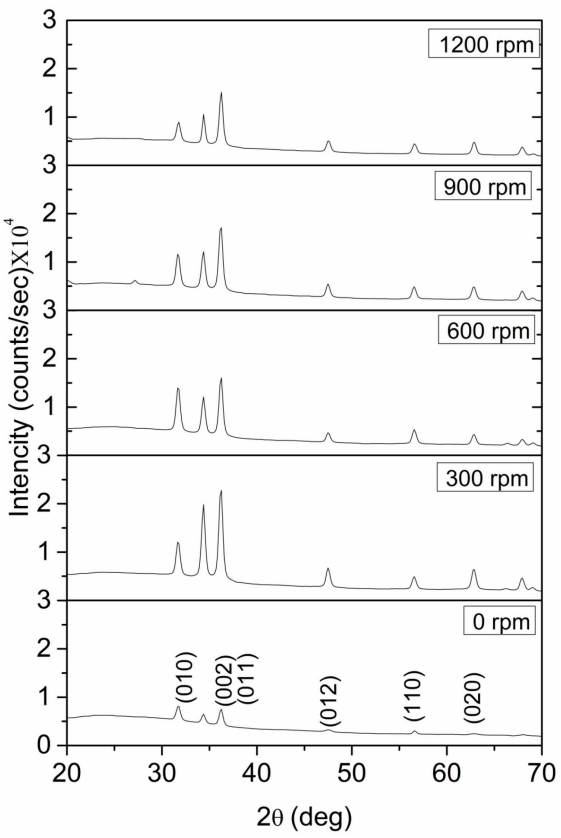

Fig. 1. XRD diffraction data of ZnO thin films obtained at different stirring rates.

TABLE II

Calculated texture coefficients at preferred orientation of ZnO films.

Exp.	rpm0	rpm300	rpm600	rpm900	rpm1200
T.C.(010)	1.298	0.617	1.147	0.888	0.376
T.C.(002)	0.919	1.479	1.048	1.143	1.330
T.C.(011)	0.782	0.902	0.803	0.968	0.991

The crystallite sizes (cs [nm]) and average crystallite sizes are given in Table III. They were calculated using the Debye–Scherrer equation

$$cs = \frac{0.089 \times 180\lambda}{314\beta\cos(\theta_C)} \tag{2}$$

where λ is the wavelength of X-ray radiation (1.54056 Å), β is the full width half maximum (FWHM), and $2\theta_C$ is the peak center [12]. It is seen in Table III that the average crystallite size of the film obtained without stirring was 16 nm. On the other hand, the average crystallite sizes of the other films were 22 nm.

3.2. Optical properties of the ZnO films

The absorbance versus wavelength was recorded by using a UV-vis spectrophotometer and absorbance plots are given in Fig. 2.

TABLE III

The crystallite sizes *cs* [nm] and energy band gaps of the ZnO films.

Exp.	cs(010) [nm]	cs(002) [nm]	cs(011) [nm]	Average cs	Band gap [eV]	Thickness [nm]
rpm0	15	15	19	16	3.97	175
rpm300	19	15	29	21	3.02	650
rpm600	19	29	19	22	3.12	650
rpm900	19	29	19	22	3.14	650
rpm1200	19	29	29	22	3.10	650

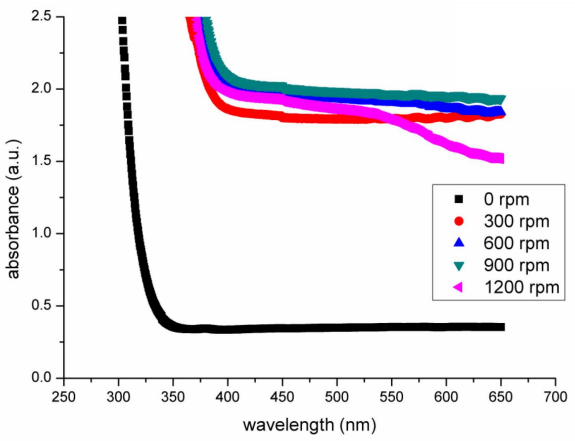

Fig. 2. Absorbance measurements at wavelengths between 300 and 650 nm.

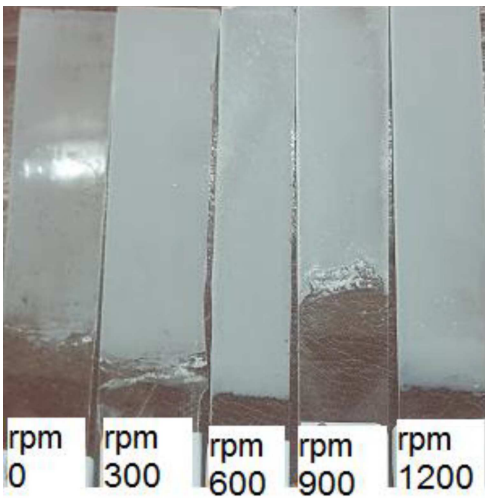

Fig. 3. The photographs of the ZnO films.

When the film thickness increased, absorbance values increased, and transparency decreased. As seen in Fig. 3, while the other films were not more transparent, that of the film obtained without stirring was quite transparent and the nanoparticles did not adhere well to the glass surface. When the other samples produced by mixing the solution were examined, it was seen that the films covered the surface quite well and formed a homogeneous and compact structure. In particular, the sample obtained at 1200 rpm appeared with covered densely by nanorods.

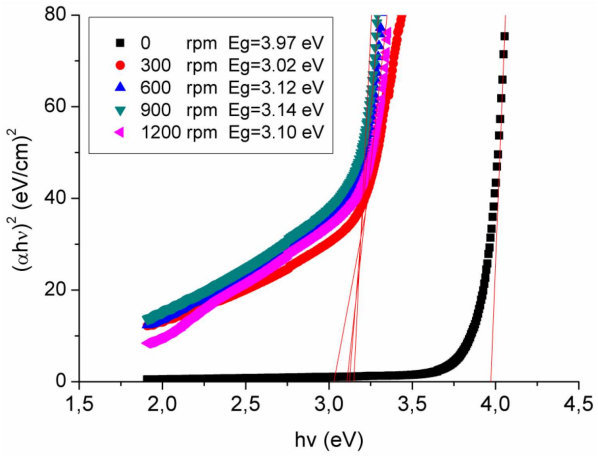

Fig. 4. The Tauc plots and energy band gaps for ZnO films.

In case of Fig. 2, the absorbance of the film obtained without stirring the solution (rpm0) was seen to be about 5 times lower than that of the other films. When rpm0 and others were compared, the sharp increasing absorbance value was quite different. The sharp increasing value of the film obtained in rpm0 was about 325 nm while the others were about 375 nm. The band gaps were strongly affected by the sharp increase of absorbance values.

The Tauc relation used to calculate the optical energy bandgap of thin films is given by

$$(\alpha h\nu)^2 = A\,(h\nu - E_g)^n\,. \tag{3}$$

In the above equation α is the absorption coefficient, $h\nu$ is the photon energy, E_g is the optical band gap of the sample, A is a constant, while $n = 1/2$ for directly allowed transitions [13].

Figure 4 shows that the energy band gap of the film obtained at rpm0 was 3.97 eV, while the average band gap for the other films was 3.10 eV. When the literature is examined, it is seen that the band gap of ZnO thin films can have different values such as 3.2, 3.3, 3.37, 3.40 eV [14–17]. The reduction of the band gap indicates that the crystallite size was increased and the film thickness was also increased, which can be seen in Table III.

3.3. FTIR of the ZnO films

The Fourier transform infrared spectroscopy (FTIR) photometer was used to investigate the vibration properties of synthesized materials [18]. In order to determine

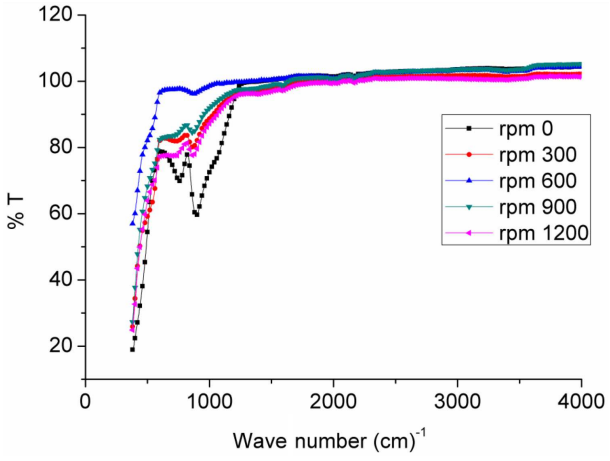

Fig. 5. FTIR spectra vs. wave number for ZnO films.

TABLE IV

Average width and average length of samples.

Exp.	Average width [nm]	Average length [nm]	Stirring rate [rev/min]
rpm0	580	3750	0
rpm300	660	3150	300
rpm600	420	2500	600
rpm900	330	1650	900
rpm1200	250	1300	1200

the structure and purity of metal nanoparticles, infrared beams were used. Metal oxides generally give absorption bands in the fingerprint region, i.e., below 1000 cm^{-1} arising from inter-atomic vibrations [19]. FTIR measurements were performed in the range of 4000 to 300 cm^{-1} wave counts. Figure 5 shows the FTIR spectra of ZnO nanoparticles. ZnO absorption stretching was observed at ≈ 900 cm^{-1} and the band at 600 cm^{-1} was the stretching mode of ZnO. Peaks observed around 593 cm^{-1} and around 925 cm^{-1} corresponded to the Zn–O vibrations. This confirmed the wurtzite structure formation of the film [20].

3.4. SEM analysis of the ZnO films

The surface morphology of ZnO thin films produced by the chemical bath deposition method was examined using scanning electroscopy (SEM). The 10000 times magnified SEM images of five different samples produced by stirring at different rates are given in Fig. 6.

It is seen from these images that the stirring rate has a significant effect on the surface properties of the films. When the stirring rate was zero, the nanorods were very rare and their length 3750 nm and diameter 580 nm. Figure 6 shows that as the stirring rate of the solutions increases, the nanorods become more frequent and their width and length decrease. The average width of these nanorods decreased to 250 nm at 1200 rpm. The smaller

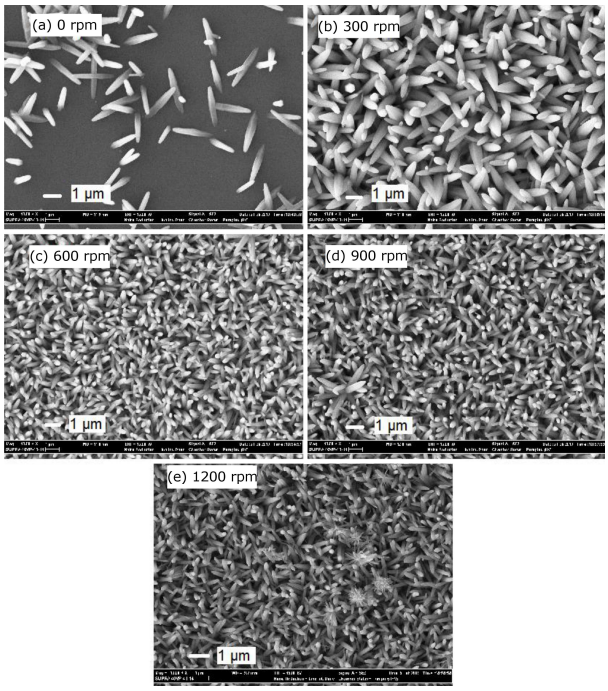

Fig. 6. SEM images of ZnO thin films magnified 10,000 times (a) 0 rpm, (b) 300 rpm, (c) 600 rpm, (d) 900 rpm, and (e) 1200 rpm.

the nanorod dimensions, the higher the surface area and the roughness, which can make the resulting thin films a suitable material for gas sensors.

The average nanorod sizes varying with stirring rates are given in Table IV. The images of SEM also show that the films obtained with stirring were dense.

4. Conclusions

In this study, the effects of the stirring rate on ZnO thin films produced by the chemical bath deposition method were investigated for the first time. When the solution was not stirred, the film had a low thickness such as 175 nm although the average of the other samples 650 nm. The structural properties were realized by using the XRD pattern. The sample obtained without stirring the solution had a low XRD peak intensity. This may be because the film was thin or the crystallization was not good. The band gaps of the films were estimated by using absorbance measurements. These plots showed a significant result. When the solution was not mixed, it was observed that the band gaps of the films were decreased up to 0.95 eV. The surface analysis was examined by SEM images. SEM images revealed that the size of nanorods was decreased as the stirring rate was increased. The photos of the surface of the obtained samples were taken. As the solution stirring rate increased, it was observed that the surfaces of the obtained samples were more densely coated and their transparency decreased. It is a known fact that the metal ions are heavier than

water molecules. Thus, when the solution was mixed, by the effect of the centrifugal force, the metal ions were thrown into the inner wall of the bath container and the surface of the glass substrate.

References

[1] J. Kathalingam, A. Ambika, N. Kim, Mr. Elanchezhiyan, J. Chae, Ys. Rhee, *Mater. Sci.* **28**, 5014 (2010).

[2] K. Ramamoorthy, M. Arivanandhan, K. Sankaranarayanan, C. Sanjeeviraja, *Mater. Chem. Phys.* **85**, 257 (2004).

[3] M.M. Ali, *J. Basrah Res.* **37**, 49 (2011).

[4] S. Masuda, K. Kitamura, Y. Okumura, S. Miyatake, H. Tabata, T. Kawai, *J. Appl. Phys.* **93**, 1624 (2003).

[5] A. Sholehah, A.H. Yuwono, C.R. Rimbani, *Mater. Sci. Forum* **737**, 28 (2013).

[6] A. Kolodziejczak-Radzimska, T. Jesionowski, *Materials (Basel)* **7**, 2833 (2014).

[7] S. Temel, F.O. Gokmen, E. Yaman, *Eur. Sci. J. (ESJ)* **13**, 28 (2017).

[8] P.B. Taunk, R. Das, D.P. Bisen, R.K. Tamrakar, N. Rathor, *Karbala Int. J. Mod. Sci.* **1**, 159 (2015).

[9] H. Khallaf, G. Chai, O. Lupan, H. Heinrich, S. Park, A. Schulte, L. Chow, *J. Phys. D Appl. Phys.* **42**, 135304 (2009).

[10] M.J. Kim, C. Kim, S.H. Sohn, *Mol. Cryst. Liq. Cryst.* **677**, 81 (2018).

[11] Y. Zhang, X.Y. Dang, J. Jin, T. Yu, B.Z. Li, Q. He, F.Y. Li, Y. Sun, *Appl. Surf. Sci.* **256**, 6871 (2010).

[12] R. Bhowmik, M.N. Murty, E.S. Srinadhu, *PMC Phys. B* **1**, 20 (2008).

[13] Rahul, A.K. Verma, R.S.N. Tripathi, S.R. Vishwakarma, *Natl. Acad. Sci. Lett.* **35**, 367 (2012).

[14] M.R. Khelladi, L. Mentar, M. Boubatra, A. Azizi, *Mater. Lett.* **67**, 331 (2012).

[15] Z. Yuan, *J. Electron. Mater.* **44**, 1187 (2015).

[16] K.L.P. Thi, L.T. Nguyen, N.H. Ke, D.A. Tuan, T.Q.A. Le, L.V.T. Hung, *J. Electron. Mater.* **47**, 6302 (2018).

[17] G.S.A. Lghamdi, A.Z.A. Lzahrani, *Middle East J. Sci. Res.* **13**, 1144 (2013).

[18] Z.R. Khan, M.S. Khan, M. Zulfequar, M. Shahid Khan, *Mater. Sci. Appl.* **02**, 340 (2011).

[19] R. Kumar, H. Rani, *Int. Lett. Chem. Phys. Astron.* **14**, 26 (2013).

[20] T. Hurma, *J. Mol. Struct.* **1189**, 1 (2019).